Three concomitant C-C dissociation pathways during the mechanical activation of an N-heterocyclic carbene precursor

DOI:
10.1038/s41557-020-0509-1

Document Version
Accepted author manuscript

Three concomitant C-C dissociation pathways during the mechanical activation of a N-heterocyclic carbene precursor

Robert Nixon and Guillaume De Bo*

Department of Chemistry, University of Manchester, Oxford Road, Manchester M13 9PL, United Kingdom
*e-mail: guillaume.debo@manchester.ac.uk.

Chemical reactions usually proceed through radical, concerted, or ionic mechanisms, yet transformations in which these three mechanisms take place at the same time are rare. In polymer mechanochemistry a mechanical force, transduced along polymer chains, is used to activate covalent bonds in mechanosensitive molecules (mechanophores). Cleavage of a C–C bond often follows a homolytic pathway but some mechanophores have also been designed that react in a concerted or, more rarely, a heterolytic manner. Here, using ^{1}H- and ^{19}F-nuclear magnetic resonance spectroscopy in combination with deuterium labelling, we show that the dissociation of a mechanophore built around an N-heterocyclic carbene precursor proceeds with the rupture of a C–C bond through concomitant heterolytic, concerted, and homolytic pathways. The distribution of products likely arises from a post-transition-state bifurcation in the reaction pathway, and their relative proportion is dictated by the polarisation of the scissile C–C bond.

Mechanical scission of covalent bonds usually occurs in a homolytic fashion [1,2] although mechanophores can be designed to react in a concerted [3] or, more rarely, heterolytic fashion [4-10]. Perhaps the most interesting aspect of polymer mechanochemistry comes from the fact that molecules under tension follow reaction pathways that can significantly deviate from their zero-force mechanism and lead to unexpected outcomes[2]. This deviation can be expressed in the nature of the product formed, such as in the electrocyclic ring openings of strained cycles along a symmetry forbidden pathway, [11] [12] and/or in the nature of the reactive intermediates [13,14], or even in the change of the rate-determining step itself [15,16] [17]. Here we show that the ultrasound-induced dissociation of a neutral N-heterocyclic carbene precursor proceeds with the rupture of a single C-C bond via concomitant heterolytic, concerted, and homolytic dissociation pathways.

N-heterocyclic carbenes (NHC) form a versatile group of stable carbenes that have found many applications in the chemical sciences, most notably as ligands in metal-based catalysts[18]. The activation of Ag- [19], Ru- [20], and Cu-based [21] mechanocatalysts, as well as a Pd-centered [22] mechanobase, have been recently reported and proceed via the dissociation of the metal-NHC bond. Interestingly, NHCs also display excellent catalytic performances on their own, and they have been used in a variety of organic transformations [23] and polymerizations [24]. We envisioned the possibilty of untapping the catalytic potential of a metal-free NHC precursor via the mechanical cleavage of a C-C bond. Several methods exist to thermally liberate a carbene from an otherwise stable precursor [25]. For example, NHCs can form stable adducts with fluorinated aromatics, which dissociate thermally via a concerted pathway [26]. We hypothesized that this reaction could be initiated mechanically from polymer **1** in which the NHC-precursor mechanophore is appended with two poly(tetrahydrofuran) (PTHF) arms (Fig. 1), one attached to the imidazolidine unit and the other to the tetrafluoroaromatic leaving group (PTHF was chosen for its ratio of chain length to molecular weight, and its lack of reactive functional groups). This design ensures the positioning of the mechanophore in the central region of the polymer where tension accumulates during sonication [2]. Constrained Geometry Simulates External Force (CoGEF) calculations [27] (DFT B3LYP/6-31G*) confirmed the suitability of this architecture by predicting the rupture of the desired C-C bond at a force (F_{max}) of 4.8 nN (Fig. 2).

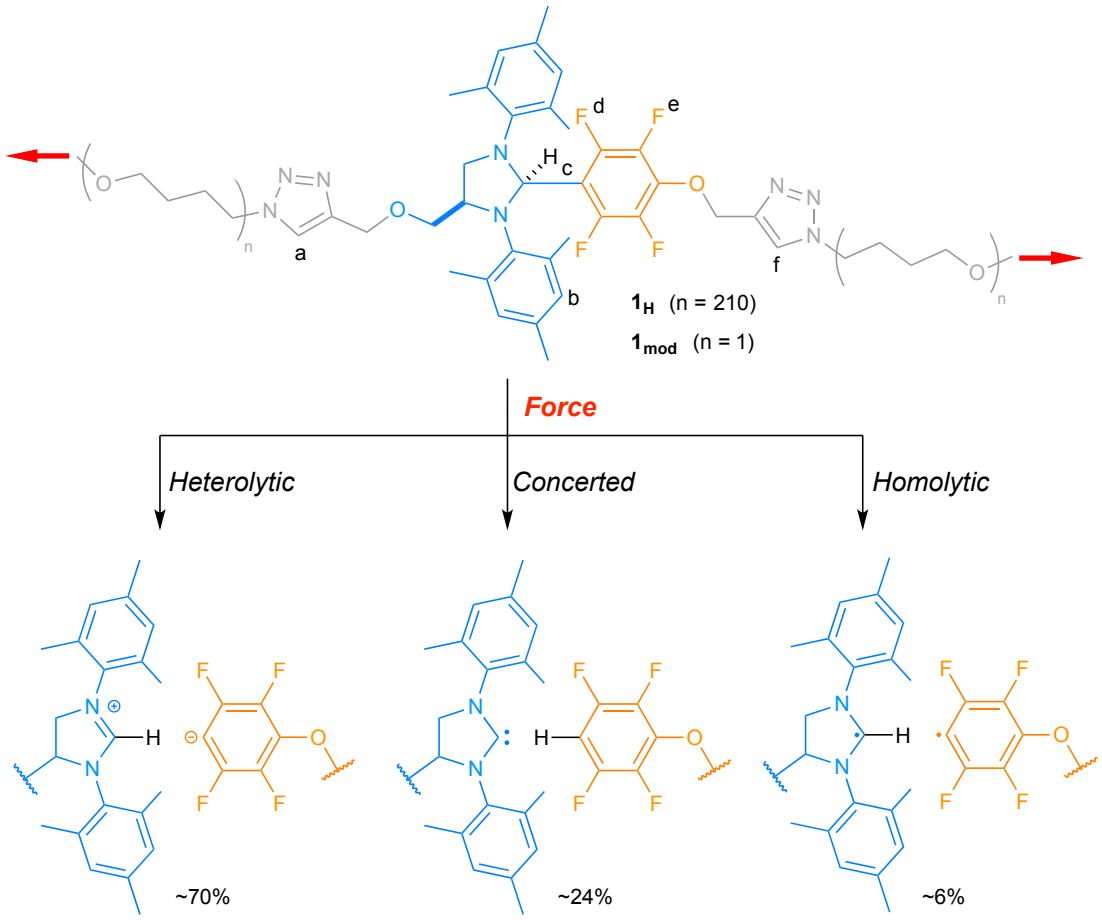

Figure 1 | The ultrasound activation of N-heterocyclic carbene precursor $\mathbf{1_H}$ proceeds via three concomitant dissociation pathways. ^{1}H- and ^{19}F-NMR, and deuterium labelling experiments reveals that most mechanophores undergo a heterolytic cleavage (~70%), followed by concerted (~24%), and homolytic (~6%) dissociations.

Results and discussion

Synthesis

Alkyne-functionalized precursor $\mathbf{2_H}$ was obtained as a single *cis*-configured diastereoisomer (Fig. 2a,c), by condensing diamine **S2** with tetrafluorobenzaldehyde **S3**, while azide-terminated polymer **3** is the result of a cationic ring-opening polymerisation (ROP)[28] of THF initiated from methyl triflate (Fig. 2a). Formation of **1**, by copper-catalyzed azide-alkyne cycloaddition (CuAAC)[29], was evidenced by the appearance of two distinctive 1,4-triazole signals (H_f, 7.57 ppm; H_a, 7.40 ppm) in the ^{1}H-nuclear magnetic resonance (NMR) spectrum (Fig. 3), and a new high-mass peak in gel permeation chromatography (GPC), indicative of a doubling in the molecular weight relative to the azide-functionalized polymer (Fig. 2b).

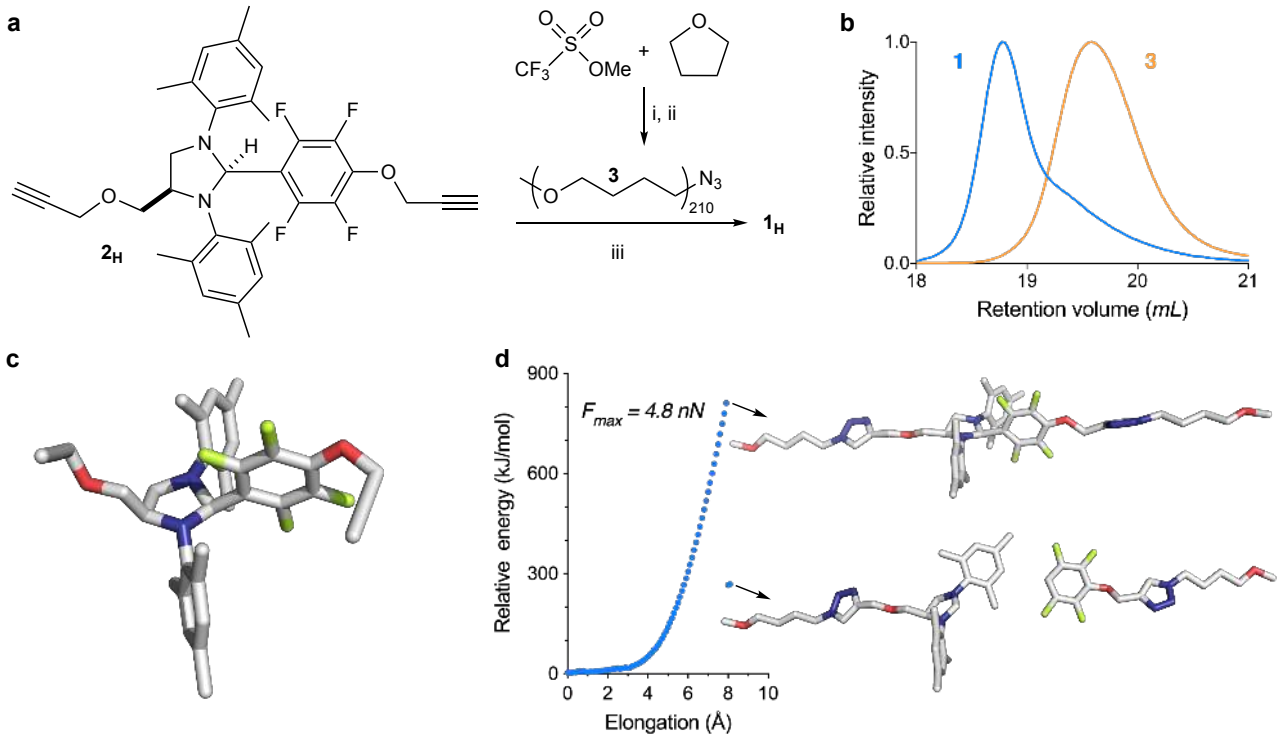

Figure 2 | Synthesis and CoGEF simulation of mechanophore-containing polymer 1. **a**, Polymer $\mathbf{1_H}$ was obtained by CuAAC of mechanophore $\mathbf{2_H}$ and PTHF **3**. Conditions: i) MeOTf (1 eq.), THF (1500 eq.), 0 ˚C, 5h, then LiBr (30 eq.). ii) NaN_3 (30 eq.), THF/DMF, 24h, rt. iii) CuBr, N,N,N',N'',N''-pentamethyldiethyltriamine, CH_2Cl_2, 48h, rt. **b**, GPC traces of polymer $\mathbf{1_H}$ ($M_{n,\,GPC}$ = 78 kDa, $Đ$ = 1.12) and **3** ($M_{n,\,NMR}$ = 15 kDa, $M_{n,\,GPC}$ = 47 kDa, $Đ$ = 1.12) (THF, 1mL/min). **c**, Solid-state structure showing the *cis* configuration of mechanophore $\mathbf{2_H}$. Hydrogen atoms omitted for clarity. C, grey; N, blue; O, red; F, green. **d**, CoGEF simulation on model $\mathbf{1_{mod}}$ (n=1) predicts the rupture of the desired C-C bond. Structures a maximal elongation (E_{max}) and after scission shown. Hydrogen atoms omitted for clarity. C, grey; N, blue; O, red; F, green.

Mechanical activation of $\mathbf{1_H}$

Activation of $\mathbf{1_H}$ was carried out in solution using high-intensity ultrasound (US) while keeping the temperature of the solution between 5 and 10 °C. Monitoring the reaction by GPC indicates the disappearance of the peak corresponding to the mechanophore-centered polymer and the appearance of a peak corresponding to half the initial M_n (Fig. 3b). If the fragmentation occurs along the predicted scissile

bond, the residual chains should contain an imidazolidine derivative (**4**) and a tetrafluorobenzene unit (**5$_H$**) respectively (Fig. 3a). This picture was confirmed by ^{1}H NMR (Fig. 3c) with the decrease in intensity of the imidazolidine proton (H_c, 6.29 ppm), and the shift of the mesityl aromatic protons (H_b, 6.86 and 6.72 ppm) along with formation of a new 1,4-triazole peak directly corresponding to that of **5$_H$** ($H_{f'}$, 7.69 ppm). Most convincing was the emergence of a distinctive peak (H_x, 6.78 ppm) displaying a triplet-of-triplets splitting pattern corresponding to the aromatic proton of **5$_H$**. Similar results were observed in the ^{19}F NMR spectra (Fig. 3d) where the asymmetric distribution of the peaks of the intact mechanophore (F_d, -137.37 and -149.43 ppm; F_e, -157.00 and -157.43 ppm), indicative of the locked conformation of the fluorinated aromatic in the mechanophore (Fig. 2c), shifts towards the symmetry of the formed tetrafluorobenzene peaks ($F_{d'}$, -140.20 ppm; $F_{e'}$, -156.22 ppm) as the mechanophore is cleaved. Control experiments, where the mechanophore is placed at the end of the polymer, confirmed the mechanical nature of the activation (see SI Section 9).

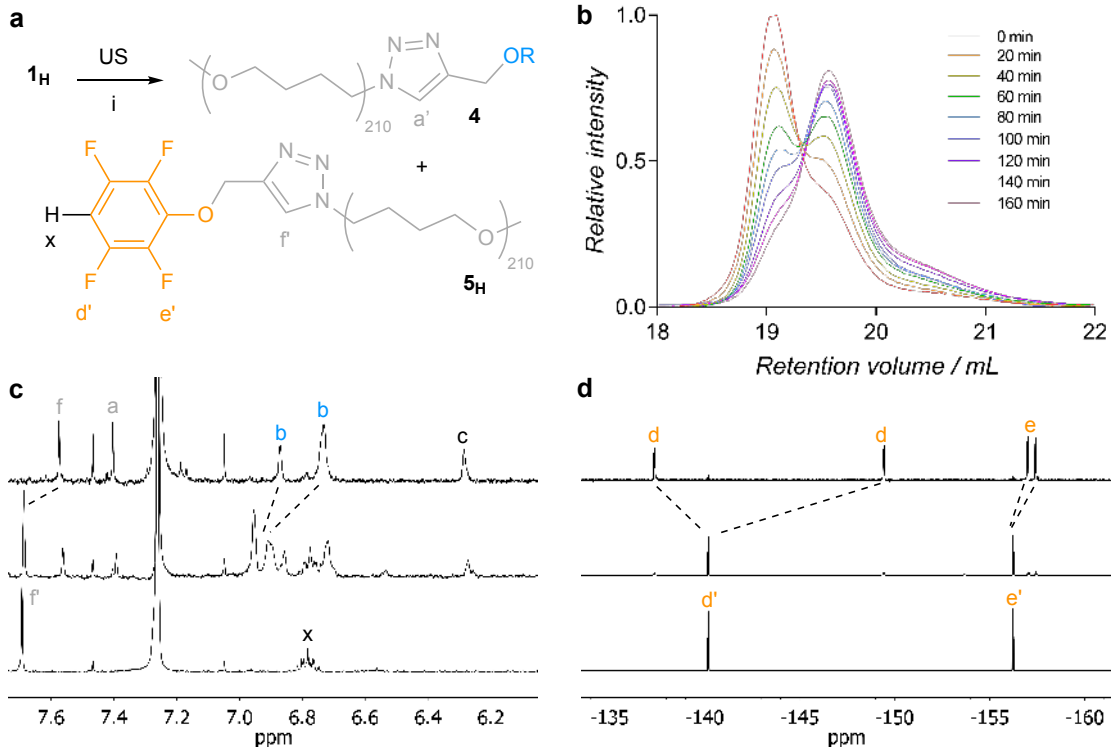

Figure 3 | Mechanical activation of polymer 1 leads to the scission of the central C-C bond. **a**, Sonication of polymer **1**. Conditions: i) US (20 KHz, 15.6 W cm^{-2}, 1 s ON / 1 s OFF), THF, 5 – 10 °C. R, imidazolidine derivative. **b**, Overlay of GPC traces gathered during sonication of polymer **1$_H$** is consistent with a rupture in

the central region of the polymer. **c**, Partial ^{1}H NMR (500 MHz, $CDCl_3$) of polymer $\mathbf{1_H}$ before (top) and after (middle) sonication along with a reference compound $\mathbf{5_{H\ ref.}}$ **d**, Partial ^{19}F NMR (376 MHz, C_6D_6) of polymer $\mathbf{1_H}$ before (top) and after (middle) sonication along with a reference compound $\mathbf{5_{H\ ref}}$ support the dissociation of the desired C-C bond. Lettering refers to assignment in Fig. 1 and Fig. 3a.

Uncovering the dissociation pathways

To further investigate the dissociation mechanism, we synthesized an analogue of $\mathbf{1_H}$ selectively deuterated at the imidazolidine position ($\mathbf{1_D}$). Indeed, cleavage of this mechanophore, through the concerted pathway required for carbene formation, would lead to movement of the deuterium atom onto the post-sonication tetrafluorobenzene structure $\mathbf{5_D}$ (Fig. 4a). ^{19}F NMR analysis of $\mathbf{1_D}$ after sonication showed two sets of peaks corresponding to both $\mathbf{5_H}$ and $\mathbf{5_D}$, indicating the cleavage was not following a single mechanism. We postulated that the cleavage of $\mathbf{1_x}$ could occur via three mechanisms: concerted, in which the free carbene is formed through transfer of the imidazolidine proton, homolytic, leading to the formation of two radicals, and heterolytic, where an imidazolinium cation and a tetrafluorophenyl anion are formed (Fig. 1).

Various sonication experiments were carried out in the presence of THF, a good hydrogen atom donor, and H_2O, a proton source, to determine the extent of formation of $\mathbf{5_H}$ and $\mathbf{5_D}$ and, by there, the prominence of each mechanism (Fig. 4). The first such experiment involved the activation of $\mathbf{1_H}$ in a solution of THF with D_2O added (Fig. 4, Entry 1), in which any amount of $\mathbf{5_D}$ formed would originate from a heterolytic mechanism in which the basic tetrafluorophenyl anion is deuterated. In these conditions, ~68% of the total amount of **5** formed incorporated a D atom ($\mathbf{5_D}$) suggesting the majority pathway is heterolytic. The extent the concerted mechanism was probed in a similar experiment where the imidazolidine ring of deuterated polymer $\mathbf{1_D}$ is the sole source of deuterium for formation of $\mathbf{5_D}$ (Fig. 4, Entry 2). This pathway was shown to occur for ~24% of the mechanophore units. Finally, we investigated the potential of a homolytic pathway, through sonication of $\mathbf{1_H}$ in fully deuterated THF-d_8 and H_2O ensuring the only source of deuterium is the THF solvent (Fig. 4, Entry 3), which is unlikely to react with the heterolytically-formed anion before H_2O does. This reaction showed a small amount of $\mathbf{5_D}$ forming (~6%). A radical trapping experiment confirms the

formation of radical species (See SI Section 8.4). Additional experiments, where H and D sources are inverted compared to Entry 1-3, show opposite $\mathbf{5_H/5_D}$ ratios (see SI Section 8.5).

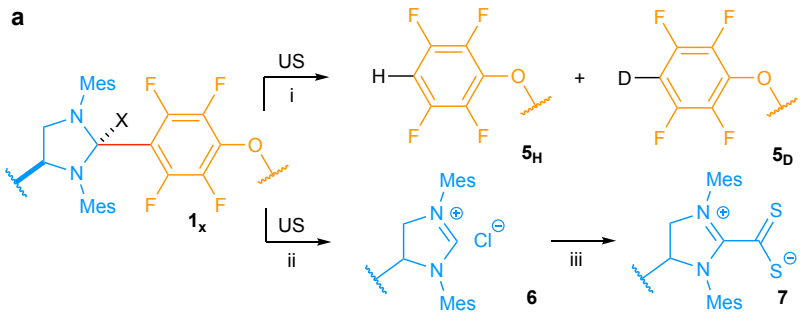

Entry	*X*	*Solvent*	$5_H/5_D$	5_D *origin*
1	H	THF/D_2O	32/68	*Heterolytic*
2	D	THF/H_2O	76/24	*Concerted*
3	H	$THF\text{-}d_8/H_2O$	95/5	*Homolytic*

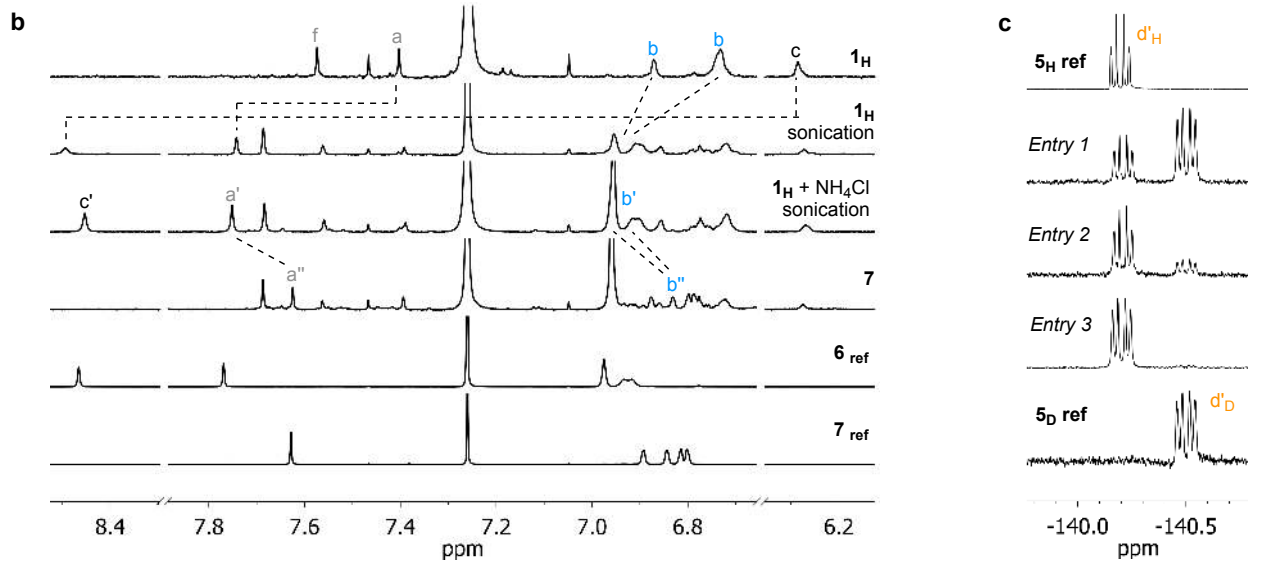

Figure 4 | Deuterium labelling experiments reveal three dissociation pathways. a, Polymer **1** cleaves to form $\mathbf{5_H}$ and $\mathbf{5_D}$ in ratios dependent upon the reaction conditions; during heterolytic cleavage an imidazolidinium species is also formed which can be deprotonated and reacted further with carbon disulfide. Conditions: i) US (20 KHz, 15.6 W cm^{-2}, 1 s ON / 1 s OFF), see Table for solvent systems, 5-10 °C. ii) US (20 KHz, 15.6 W cm^{-2}, 1 s ON / 1 s OFF), NH_4Cl, THF, H_2O, 5-10 °C. iii) NaH, CS_2, THF, 1 h, rt. Mes, mesityl group. **b**, Partial ^1H NMR (500 MHz, $CDCl_3$) of polymer $\mathbf{1_H}$ before ($\mathbf{1_H}$) and after ($\mathbf{1_H}$ sonication) sonication in THF and after sonication under conditions (ii) ($\mathbf{1_H}$ + NH_4Cl sonication) followed by reaction under conditions (iii) (**7**), along with reference compounds ($\mathbf{6_{ref}}$ and $\mathbf{7_{ref}}$). **c**, Partial ^{19}F NMR (376 MHz, C_6D_6) of sonication reactions, corresponding to entries in the table along with reference compounds $\mathbf{5_{H\ ref}}$ and $\mathbf{5_{D\ ref}}$, is used to

determine the extent of deuterium incorporation in the tetrafluorobenzene dissociation product. Lettering refers to assignment in Fig. 1 and Fig. 3a.

Considering the concomitant existence of three different dissociation pathways, one could expect to observe a complex mixture of products deriving from the imidazolidine section of the mechanophore. However, the aromatic region of the ^{1}H NMR spectrum presents a relatively simple pattern (Fig. 4b), which is characterized by the appearance a broad peak around 8.5 ppm, suggestive of an imidazolinium proton, and an equally intense peak at 7.74 ppm likely corresponding to a new triazole species. Though hydrolysis of the post-cleavage species could also be possible during sonication, resulting in similarly shifted peaks in the ^{1}H NMR, we confirmed this was not the case through comparison with reference amide compounds (Supplementary Fig. 12). In fact, comparison with reference $\mathbf{6}_{\mathbf{ref}}$ (Fig. 4b) further confirmed that the imidazolium salt is the end product for the imidazolidine side of the mechanophore, either formed directly upon heterolytic cleavage or after reprotonation of the carbene generated in the concerted pathway. Interestingly, we were able to select the counterion of the imidazolium cation upon addition of various salts during the sonication. Adding NH_4Cl resulted in the imidazolidinium chloride salt **6** whereas addition of LiBr lead to the bromide salt (see SI section 8.3). In the absence of added salt, a chloride anion is the most likely counterion (probably originating from brine washes during the PTHF synthesis). To further confirm the existence of this salt species we decided to test its reactivity by treating the sonicated polymer with NaH to generate the carbene [18], which was trapped *in situ* with CS_2 to afford zwitterionic compound **7** (Fig. 4b and Supplementary Fig. 11).

Controlling the dissociation pathways

We were intrigued by the possibility of influencing the preferred reaction pathway by altering the polarisation of the scissile C-C bond. Since the electron-poor tetrafluorophenyl derivative favours the heterolytic pathway, due to its ability to stabilise a negative charge, we hypothesised that reducing the polarisation of the scissile C-C bond could favour the formation of the carbene via the concerted pathway.

Mechanical activation of thermally inert (see SI section 7) mono- and difluoro adducts, **8b** and **8a** respectively (Fig. 5a), indicate that a decrease in the electron-withdrawing ability of the departing aromatic favours the concerted pathway (Fig. 5b). This trend culminates with monofluoro mechanophore **8b**, which produces 75% of concerted products (Fig. 5c).

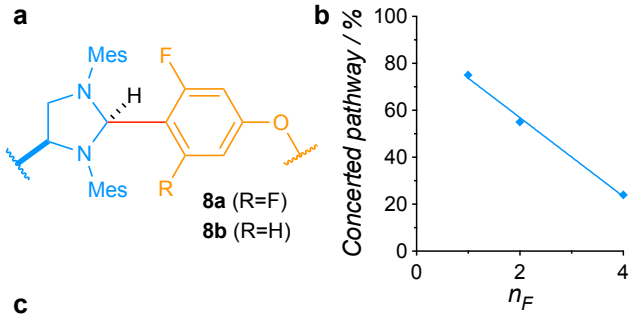

c

Adduct	n_F	***Heterolytic***	***Concerted***	***Homolytic***
1_H	4	*70%*	*24%*	*6%*
8a	2	*45%*	*55%*	*n.o.*
8b	1	*25%*	*75%*	*n.o.*

Figure 5 | Scissile bond polarisation controls the relative importance of each dissociation pathway. a, Structure of mono- and difluoro adducts **8b** and **8a**. Mes, mesityl group. **b**, Proportion of the mechanophore cleaving in a concerted pathway as a function of the number of fluorine atoms (n_F) in the aromatic leaving group. **c**, Relative importance of each dissociation pathway observed during the sonication of adducts **1_H**, **8a**, and **8b** (n.o.: not observed; see SI for conditions).

Dissociation mechanism

The question arises of what is the nature of the mechanism leading to these three concomitant dissociation pathways. The divergent pathways could result from up to three different but energetically close TS, or from a post-TS bifurcation where the potential energy surface (PES) is modified by force to allow divergent reaction pathways to emerge (Fig. 6a). In the absence of external force, the generation of the carbene species via a concerted mechanism is favoured. However, it has been shown that the rate of thermal activation of similar adducts is sensitive to the solvent polarity, suggesting a significant degree of

asynchronicity in the transition state.[30] This picture is confirmed by the calculated geometry of the TS (B3LYP/6-31G*) during the force-free concerted elimination of the tetrafluoroarene in model **S25** (see SI Section 10.2). The C^1-C^2 bond presents a large degree of dissociation with partial positive and negative charges accumulating at C^1 and C^2 respectively. Interestingly, a very similar geometry is observed in the stretched mechanophore at E_{max} (Fig. 2d), suggesting that external tension should not negatively impact the TS of the concerted pathway. At the same time, heterolytic cleavage is the main dissociation pathway when the bond is highly polarised (n_F = 4), and it is also predicted in the CoGEF calculations (see Supplementary Fig. 19). Under tension, the reaction coordinate is restricted to the elongation of C^1-C^2 and C^1-H along the force vector and, as such, the heterolytic scission should follow a similar pathway to the concerted dissociation except for the fact that C^1-C^2 scission occurs before the proton transfer. In fact force-modified PES calculations reveal a bifurcating surface with two trajectories originating from a single TS (Fig. 6b-d).[31,32] With model **R** (X=F, n_F=4), a shorter version of the E_{max} structure in Fig. 2d, the reaction follows a single pathway along a channel centred on C^1-H=1.09Å and culminating at the TS around C^1-C^2=2.15Å. Beyond this point the reaction can either proceed along the same trajectory to reach the heterolytic products, or bifurcate to another valley of the PES where the C^1-C^2 and C^1-H bonds extend at a similar rate to generate the concerted products (Fig. 6c and SI Section 10.3). At low force (~0.1nN), the heterolytic channel almost completely disappears from the PES (Fig. 6b). Similarly, decreasing the polarisation of the scissile bond (n_F=2) improves the synchronicity of the dissociation and reduces the importance of the heterolytic pathway (Fig. 6d). The emergence of a post-TS bifurcation in a force-modified PES has been recently observed in other mechanophores,[33,34] and could be a common phenomenon in mechanochemical transformations. Since the minor homolytic pathway is not observed when the importance of the heterolytic pathway decreases (Fig. 5b), it seems plausible that these two pathways are linked and that the homolytic pathway results from an electron transfer during the formation of the heterolytic products.

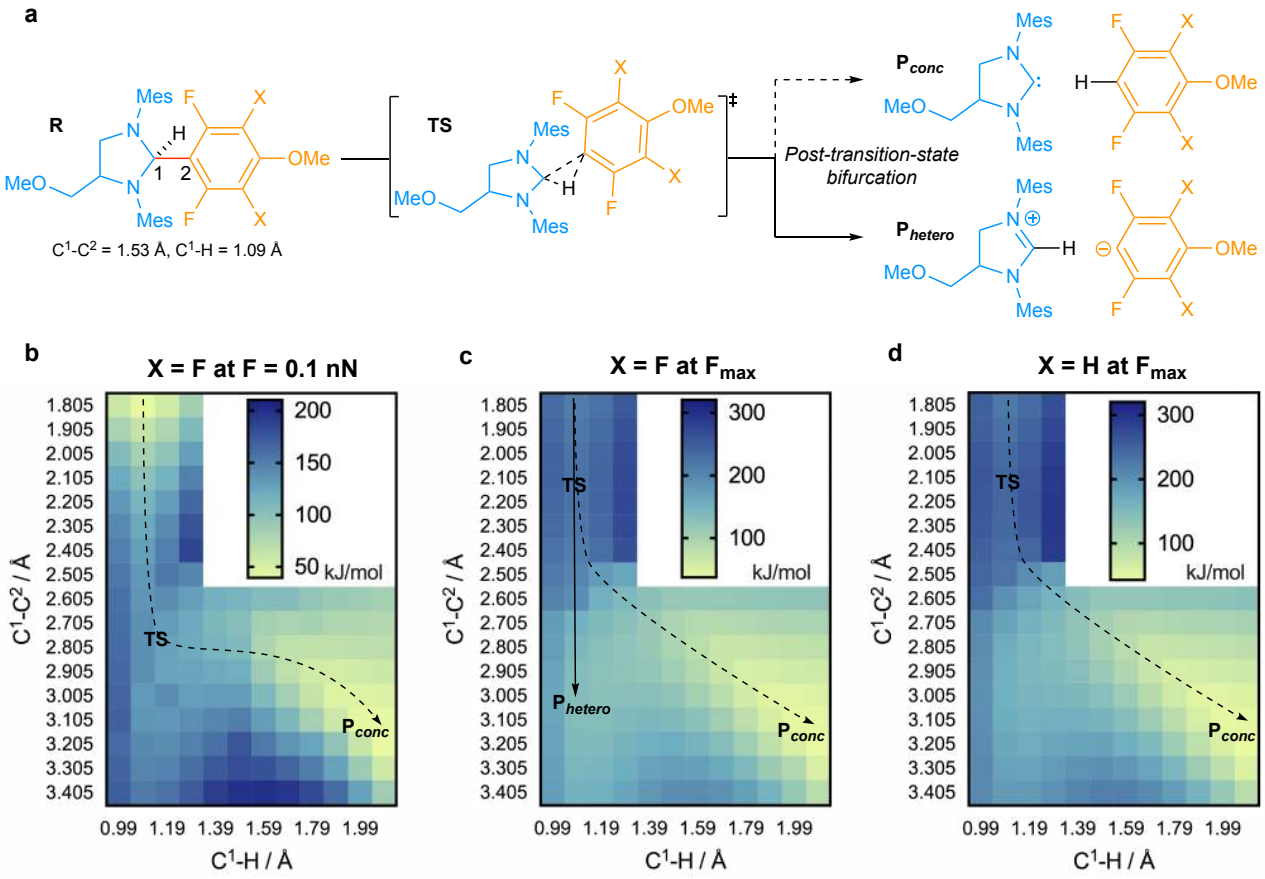

Figure 6 | The main dissociation pathways are likely the result of a post-transition-state bifurcation on the force-modified potential energy surface. a, Proposed mechanism for the mechanical cleavage of C^1-C^2 bond leading to concerted and heterolytic products. Mes, mesityl group. Me, methyl group. **b**, PES (B3LYP/6-31G*) for the dissociation of C^1-C^2 in **R** (X=F) at low force (constrained Me-Me distance of 12.249Å, corresponding to the intermediate at 3.1Å in CoGEF of $\mathbf{1}_{mod}$ in Fig. 2d). **c**, PES (B3LYP/6-31G*) for the dissociation of C^1-C^2 in **R** (X=F) at F_{max} (constrained Me-Me distance of 13.839Å, corresponding to the E_{max} intermediate in CoGEF of $\mathbf{1}_{mod}$ in Fig. 2d). **d**, PES (B3LYP/6-31G*) for the dissociation of C^1-C^2 in **R** (X=H) at F_{max} (constrained Me-Me distance of 13.839Å, corresponding to the E_{max} intermediate in CoGEF of **8a'** in Supplementary Fig. 19). The relative energy of each intermediate was determined by setting the energy of the force-free state (**R**) at 0 kJ/mol. Plain and dashed lines indicate heterolytic and concerted pathways respectively. The energy values associated with the heterolytic pathway are probably overestimated due to the lack of a solvent model.

Conclusions

In conclusion, we have uncovered the presence of three concomitant dissociation pathways (heterolytic, concerted, and homolytic) for the rupture of a C-C bond upon mechanochemical activation of a N-heterocyclic carbene precursor, and found that the relative proportion of each pathway is dictated by the polarisation of the scissile C-C bond. In the tetrafluoro mechanophore, the major pathway (~70%) is a heterolytic scission that results in an anionic species, that is readily protonated, and a cationic imidazolidinium species that persists as an isolable chloride salt. ^{19}F NMR analysis, combined with strategic deuteration of the mechanophore, shows the presence of a concerted pathway (~24%) that results in formation of a free carbene species. A third, minor pathway (~6%) leads to the formation of radical species by homolytic cleavage. When the polarisation of the scissile C-C bond decreases, the concerted pathway becomes dominant. This trend culminates with a monofluoro mechanophore, which produces 75% of the concerted products. The product distribution is likely the result of a post-transition-state bifurcation on the force-modified potential energy surface. This phenomenon has been recently observed in other mechanochemical transformations, [33,34] and might be more common than anticipated. Interestingly, the shape of the force-modified PES can be altered to favour a particular dissociation pathway by tuning the electronic properties of the mechanophore. These results further demonstrate the vast potential offered by polymer mechanochemistry to expand the reactivity space by favouring unusual reaction pathways. The possibility to probe and alter these reaction pathways, using labeling experiments and substituent effects respectively, should help refine the current models of reactivity for molecules under tension and provide new ways to control the outcome of a mechanochemical reaction.

References

1. Beyer, M. K. & Clausen-Schaumann, H. Mechanochemistry: the mechanical activation of covalent bonds. *Chem. Rev.* **105,** 2921–2948 (2005).
2. Caruso, M. M. *et al.* Mechanically-induced chemical changes in polymeric materials. *Chem. Rev.* **109,** 5755–5798 (2009).

3. Izak-Nau, E., Campagna, D., Baumann, C. & Göstl, R. Polymer mechanochemistry-enabled pericyclic reactions. *Polym. Chem.* **11,** 2274–2299 (2020).

4. Klukovich, H. M. *et al.* Tension Trapping of Carbonyl Ylides Facilitated by a Change in Polymer Backbone. *J. Am. Chem. Soc.* **134,** 9577–9580 (2012).

5. Shiraki, T., Diesendruck, C. E. & Moore, J. S. The mechanochemical production of phenyl cations through heterolytic bond scission. *Faraday Discuss.* **170,** 385–394 (2014).

6. Diesendruck, C. E. *et al.* Mechanically triggered heterolytic unzipping of a low-ceiling-temperature polymer. *Nat. Chem.* **6,** 623–628 (2014).

7. Peterson, G. I. & Boydston, A. J. Kinetic Analysis of Mechanochemical Chain Scission of Linear Poly(phthalaldehyde). *Macromol. Rapid Comm.* **35,** 1611–1614 (2014).

8. Di Giannantonio, M. *et al.* Triggered Metal Ion Release and Oxidation: Ferrocene as a Mechanophore in Polymers. *Angew. Chem. Int. Ed.* **57,** 11445–11450 (2018).

9. Sha, Y. *et al.* Quantitative and Mechanistic Mechanochemistry in Ferrocene Dissociation. *ACS Macro Lett.* 1174–1179 (2018).

10. Sha, Y. *et al.* Generalizing metallocene mechanochemistry to ruthenocene mechanophores. *Chem. Sci.* **10,** 4959–4965 (2019).

11. Hickenboth, C. R. *et al.* Biasing reaction pathways with mechanical force. *Nature* **446,** 423–427 (2007).

12. Wang, J. *et al.* Inducing and quantifying forbidden reactivity with single-molecule polymer mechanochemistry. *Nat. Chem.* **7,** 323–327 (2015).

13. Lenhardt, J. M. *et al.* Trapping a Diradical Transition State by Mechanochemical Polymer Extension. *Science* **329,** 1057–1060 (2010).

14. Wang, J., Kouznetsova, T. B. & Craig, S. L. Reactivity and Mechanism of a Mechanically Activated anti-Woodward–Hoffmann–DePuy Reaction. *J. Am. Chem. Soc.* **137,** 11554–11557 (2015).

15. Garcia-Manyes, S., Liang, J., Szoszkiewicz, R., Kuo, T.-L. & Fernández, J. M. Force-activated reactivity switch in a bimolecular chemical reaction. *Nat. Chem.* **1,** 236–242 (2009).

16. Tian, Y., Kucharski, T. J., Yang, Q.-Z. & Boulatov, R. Model studies of force-dependent kinetics of multi-barrier reactions. *Nat. Commun.* **4,** 2538 (2013).

17. Pill, M. F., East, A. L. L., Marx, D., Beyer, M. K. & Clausen-Schaumann, H. Mechanical Activation Drastically Accelerates Amide Bond Hydrolysis, Matching Enzyme Activity. *Angew. Chem. Int. Ed.* **58,** 9787–9790 (2019).

18. Hopkinson, M. N., Richter, C., Schedler, M. & Glorius, F. An overview of N-heterocyclic carbenes. *Nature* **510,** 485–496 (2014).

19. Sijbesma, R. P., Karthikeyan, S., Potisek, S. L. & Piermattei, A. Highly efficient mechanochemical scission of silver-carbene coordination polymers. *J. Am. Chem. Soc.* **130,** 14968–14969 (2008).

20. Piermattei, A., Karthikeyan, S. & Sijbesma, R. P. Activating catalysts with mechanical force. *Nat. Chem.* **1,** 133–137 (2009).

21. Michael, P. & Binder, W. H. A Mechanochemically Triggered 'Click' Catalyst. *Angew. Chem. Int. Ed.* **54,** 13918–13922 (2015).

22. Clough, J. M., Balan, A., van Daal, T. L. J. & Sijbesma, R. P. Probing Force with Mechanobase-Induced Chemiluminescence. *Angew. Chem. Int. Ed.* **55,** 1445–1449 (2016).

23. Flanigan, D. M., Romanov-Michailidis, F., White, N. A. & Rovis, T. Organocatalytic Reactions Enabled by N-Heterocyclic Carbenes. *Chem. Rev.* **115,** 9307–9387 (2015).

24. Naumann, S. & Dove, A. P. N-Heterocyclic carbenes as organocatalysts for polymerizations: trends and frontiers. *Polym. Chem.* **6,** 3185–3200 (2015).

25. Naumann, S. & Buchmeiser, M. R. Liberation of N-heterocyclic carbenes (NHCs) from thermally labile progenitors: protected NHCs as versatile tools in organo- and polymerization catalysis. *Catal. Sci. Technol.* **4,** 2466–2479 (2014).

26. Nyce, G. W., Csihony, S., Waymouth, R. M. & Hedrick, J. L. A General and Versatile Approach to Thermally Generated N-Heterocyclic Carbenes. *Chem. Eur. J.* **10,** 4073–4079 (2004).

27. Beyer, M. The mechanical strength of a covalent bond calculated by density functional theory. *J. Chem. Phys.* **112,** 7307–7312 (2000).

28. Dubois, P., Coulembier, O. & Raquez, J.-M. *Handbook of Ring-Opening Polymerization*. (John Wiley & Sons, 2009).

29. Meldal, M. & Tornoe, C. W. Cu-catalyzed azide-alkyne cycloaddition. *Chem. Rev.* **108,** 2952–3015 (2008).

30. Blum, A. P., Ritter, T. & Grubbs, R. H. Synthesis of N-Heterocylic Carbene-Containing Metal Complexes from 2-(Pentafluorophenyl)imidazolidines. *Organometallics* **26,** 2122–2124 (2007).

31. Hare, S. R. & Tantillo, D. J. Post-transition state bifurcations gain momentum – current state of the field. *Pure Appl Chem* **89,** 679–698 (2017).

32. Ess, D. H. *et al.* Bifurcations on Potential Energy Surfaces of Organic Reactions. *Angew. Chem. Int. Ed.* **47,** 7592–7601 (2008).

33. Chen, Z. *et al.* The cascade unzipping of ladderane reveals dynamic effects in mechanochemistry. *Nat. Chem.* (2020). doi:10.1038/s41557-019-0396-5

34. Wollenhaupt, M., Schran, C., Krupicka, M. & Marx, D. Force-Induced Catastrophes on Energy Landscapes: Mechanochemical Manipulation of Downhill and Uphill Bifurcations Explains the Ring-Opening Selectivity of Cyclopropanes. *ChemPhysChem* **19,** 837–847 (2018).

Acknowledgments

We thank the EPSRC for a studentship to R.N. and the Royal Society for a University Research Fellowship to G.D.B.

Author contributions

G.D.B. conceived the project. R.N. and G.D.B. designed the experiments. R.N. carried out the experimental work. G.D.B performed the calculations. All authors contributed to the analysis of the results and the writing of the manuscript.

Competing financial interests

The authors declare no competing financial interests.

Additional information

Supplementary information is available in the online version of the paper.

Reprints and permissions information is available online at www.nature.com/reprints.

Correspondence and requests for materials should be addressed to G.D.B.

Figures captions

Methods

See Supplementary Information for detailed methods and protocols.

Mechanical activation. The specified polymer (70 mg) was dissolved in the specified solvent mixture (15 mL) and added to a modified Suslick cell. The solution was sonicated using a Sonics VCX 500 ultrasonic processor equipped with a 13 mm diameter solid probe or replaceable-tip probe (20 KHz, 15.6 W cm^{-2}, 1 s ON / 1 s OFF, 5 – 10 °C). Nitrogen was gently bubbled through the solution as it was sonicated. After 180 min of sonication time, the mixture concentrated and dried under high vacuum for an extended period of time (approximately 24 h), the polymer was washed with acetonitrile (5 mL) before drying again.

CoGEF calculation. CoGEF calculations were performed on Spartan '14 following Beyer's method.[27] The structure of the mechanophore was built in Spartan '14 and minimized using molecular mechanics (MMFF). The distance between the terminal methyl groups of $\mathbf{1_{mod}}$ was constrained and increased by increments of 0.1 Å. At each step, the energy was minimized by molecular mechanics (MMFF) then DFT (B3LYP/6-31G*) in vacuum. The relative energy of each intermediate was determined by setting the energy of the initial state at 0 kJ/mol. F_{max} value is determined from the slope of the final 40% of the energy/elongation curve (i.e. from 0.6 E_{max} to E_{max}).

PES calculations. PES calculations were performed on Spartan '14. The structure of the model mechanophore **R** was built in Spartan '14 and minimized using molecular mechanics (MMFF). The distance

between the terminal methyl groups was constrained (D = 12.249Å (low-force) or 13.839Å (E_{max})), and C^1-C^2 and C^1-H bond lengths were increased by increments of 0.1 Å from 1.805Å to 3.405Å, and 0.99Å to 2.09Å respectively. At each step, the energy was minimized by molecular mechanics (MMFF) then DFT (B3LYP/6-31G*) in vacuum. The relative energy of each intermediate was determined by setting the energy of the force-free state at 0 kJ/mol. The energy values associated with the heterolytic pathway are probably overestimated due to the lack of a solvent model.

Data availability

Crystallographic data for the structures reported in this Article have been deposited at the Cambridge Crystallographic Data Centre, under deposition number CCDC 1991781 ($\mathbf{2_H}$). The data that support the finding of this study are available within the paper and its Supplementary Information, or are available from the figshare data repository (https://figshare.com) under doi 10.6084/m9.figshare.12156378.